Event generator for J/ψ and $\psi(2S)$ decay

J. C. Chen,[1,2] G. S. Huang,[1] X. R. Qi,[1] D. H. Zhang,[1] and Y. S. Zhu[1]
[1]*Institute of High Energy Physics, Chinese Academy of Sciences, Beijing 100039, China*
[2]*China Center of Advanced Science and Technology (World Laboratory), P.O. Box 8730, Beijing 100080, China*

(Received 13 December 1999; published 23 June 2000)

We have developed a Monte Carlo generator for simulating charmonium J/ψ and $\psi(2S)$ inclusive decay. In the model, charmonium decay via gluons is described by the QCD partonic theory, and the partonic hadronization is handled by the LUND model. Extended C- and G-parity conservation are assumed and abnormal suppression effects of charmonium decay are included. This model reproduces the properties of hadronic events in the charmonium inclusive decay, such as the branching ratios of hadronic resonance, the ratios of stable hadrons and the radiative products, and as the global properties of hadronic events.

PACS number(s): 13.25.Gv, 13.65.+i, 14.65.Dw

I. INTRODUCTION

Although the charmonium resonances J/ψ and $\psi(2S)$ were found more than 20 years ago, the study of their properties is still an active field, and a model to simulate the charmonium inclusive decay is appealing. Since charmonium was found, much theoretical effort has been made toward understanding the spectrum and decay properties of the charmonium family [1–6]. The existence of a non-Abelian gluon field is the key hypothesis of QCD, and the discoveries of glueballs and hybrids comprise direct and essential proof of the validity of QCD. It is an ideal place to search for glueballs and hybrids in the J/ψ decay process, because perturbative QCD indicates that low-lying glueballs (with spin parities 0^{2+}, 2^{2+}, and 0^{-+}) and hybrids can be produced in J/ψ decay. Therefore, systematic studies of the J/ψ and $\psi(2S)$ decay modes, and precise measurements of branching ratios, angular distributions, and other properties, are important ways to search for glueballs and hybrids. Although over 100 decay modes of J/ψ and around 30 decay modes of $\psi(2S)$ have been measured, most of their measured uncertainties are 10–30 %. In order to improve the precision of the measurements, an event generator which precisely reproduces global properties of J/ψ and $\psi(2S)$ decays is needed. This will be very important to a calculation of acceptance for hadronic-inclusive processes [for example, for measurements of the resonance cross section in $J/\psi,\psi(2S)\to$hadrons], as well as to the estimate of the background in the exclusive processes which related J/ψ and $\psi(2S)$ decay. These usually depend on simulations by the phase-space model, thus causing major systematic errors due to the obvious discrepancies between the experimental data and the Monte Carlo simulation results. This situation hinders us from conducting precise measurements. If there is a model which reproduces global properties of the charmonium-inclusive decays quantitatively, then the acceptance can be calculated with less uncertainty, and charmonium decay modes can be measured more precisely. The direct goals of our work are as follows.

(1) Study inclusive processes in the $J/\psi,\psi(2S)\to$hadrons, and provide precise calculations of the acceptance.

(2) Study exclusive processes in the $J/\psi,\psi(2S)\to$hadrons, and provide the reliable estimates of their background.

(3) Study exclusive processes in those decays which produce J/ψ or $\psi(2S)$, such as in the χ_{cJ} or Υ decays, and provide a reasonable estimate of the background.

The main characteristics of this scheme are as follows. (1) The main measured modes of charmonium decays are included in the model. (2) The flavor generation machinery of the LUND model is applied for the quark hadronization. (3) Gluon fragmentation is performed by the LUND shower string model [7]. (4) C parity and G parity conservation are included in the interactions. (5) Unstable particle decays are handled by the LUND model to produce the final states. (6) Both Particle Data Group (PDG) and Beijing spectrometer (BES) results are fully used to check and tune parameters of the model. (7) Not only the branching ratios of most modes of J/ψ and $\psi(2S)$ decays are reproduced by this generator, but the global properties of hadronic events are consistent with the experimental data, such as the charged multiplicity, Kobo-Nielsen-Olesen (KNO) scaling distribution, Feynman

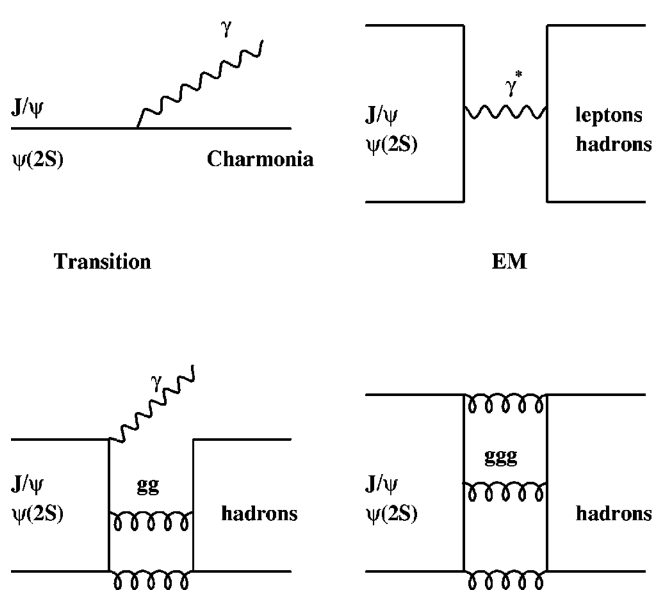

FIG. 1. Charmonia decay: $\mathrm{Br}(c\overline{c})+\mathrm{Br}(\gamma^{*})+\mathrm{Br}(\gamma gg)+\mathrm{Br}(ggg)=1$.

TABLE I. Parameters of JETSET7.4 tuned in the charmonium generator.

Dynamic parameter				Particle ratio			
Parameter	Def	Tuned	Description	Parameter	Def	Tuned	Description
$PARJ(21)$	0.36	0.5	σ, width of Gaussian	$parj(11)$	0.5	0.60	V/P ratio of $u\&d$
$PARJ(33)$	0.8	0.6	diquark minium mass	$parj(12)$	0.6	0.66	V/P ratio of s
$parj(126)$	2 GeV	1 GeV	gg minimum mass	$parj(14)$	0	0.62	axial Vector ratio
$parj(25)$	1.0	0.5	η extra suppression	$parj(15)$	0	0.12	scalar meson ratio
				$parj(16)$	0	0.12	another axial Vector
				$parj(17)$	0	0.10	tensor meson
				$parj(1)$	0.1	0.09	$p(qq)/p(q)$
				$parj(2)$	0.3	0.4	$p(ss)/p(uu)$

scaling distribution, rapidity distribution, sphericity distribution, transverse momentum distribution, and so on.

In the following, we introduce the method of the model first; then simulate J/ψ and $\psi(2S)$ decay with the generator; and compare the Monte Carlo results with experimental data from PDG and BES experiments. Section IV contains conclusions.

II. METHOD

A. Partonic production in the charmonium-inclusive decay

Figure 1 shows charmonium decay via four types of Feynman diagrams. We divide these into two categories according to whether they are completely measured or not. The first category consists of decays through transitions [such as $J/\psi\rightarrow\gamma\eta_c$ and $\psi(2S)\rightarrow J/\psi+X,\gamma\chi_{cJ},\gamma\eta_c$] and decays into lepton pairs via a virtual photon [such as, $J/\psi\rightarrow e^+e^-,\mu^+\mu^-$ or $\psi(2S)\rightarrow e^+e^-,\mu^+\mu^-,\tau^+\tau^-$]. These decay modes have been measured in many experiments, and their properties are fully listed by the PDG. In our simulation, these decay modes are included into the generator directly according to their measured branching ratios from the PDG [8–10].

The second category consists of modes which are only measured partly, such as charmonium decay into hadrons via a virtual photon, through γgg or ggg. In our model, the total branching ratios of charmonium decays into hadrons via a virtual photon are included directly by the data from the PDG [9], which are 0.17 for J/ψ and 0.029 for $\psi(2S)$. The virtual photon decaying into hadrons via $q\bar{q}$ is performed by the JETSET7.4 generator.

As to charmonium decay into hadrons via γgg or ggg, their properties have been fully studied by many theorists [11–13,4,14]. According to QCD, the $J^{PC}=1^{2-}$ states should decay primarily into three gluons or two gluons together with a photon, but the latter is suppressed by a factor α_{em}/α_s. Brodsky *et al.* [14] proved that, to order a_s^2, the branching ratio for a quarkonia into γgg or ggg follows the relation

$$\Gamma(q\bar{q}(1S)\rightarrow gg\gamma)/\Gamma(q\bar{q}(1S)\rightarrow ggg) =\frac{36e_q^2}{5}\frac{\alpha_{em}}{\alpha_s}\left\{1+(2.2\pm0.6)\frac{\alpha_s}{\pi}\right\}. \tag{1}$$

In the J/ψ decay, the value of this ratio is about 10% [5]. The fractional energies of γgg or ggg, $x_i=2E_i/E_{CM}$, are given by Eq. (2) [11,12,4]:

$$\frac{1}{\sigma_{ggg}}\frac{d\sigma_{ggg}}{dx_1dx_2}=\frac{1}{\pi^2-9}\left\{\left(\frac{1-x_1}{x_2x_3}\right)^2+\left(\frac{1-x_2}{x_1x_3}\right)^2+\left(\frac{1-x_3}{x_1x_2}\right)^2\right\}. \tag{2}$$

For massless gluon and photon, the values of x_i(i=1,2,3) are with the region

$$0\leqslant x_i\leqslant 1, \tag{3}$$

and satisfies

$$x_1+x_2+x_3=2. \tag{4}$$

To a high accuracy, Eq. (2) can be approximated by Eq. (5) [11]:

TABLE II. Ratio of $J/(J+1/2)$, $I/(I+1)$.

Particle	$\pi^\pm$	$a_2^\pm$	Λ	Σ	Σ^*	Ξ	Δ	K	K^*	K_1
R_J^i	0	0	0.07	0.15	0.2	0.7	0.7	0.3	0.6	0.7
Particle	K_0^*	K_1^*	K_2^*	n	p					
R_J^i	0.7	0.7	0.	0.9	0.9					
Particle	gamma	n	p							
R_I^i	0.5	0.02	0.02							

TABLE III. Branching ratios added in the J/ψ decay.

mode	$\rho\pi$	$a_2\pi$	$a_2\rho$	$\omega\eta$	ωf_2	$p\bar{p}\omega$	$b_1^0\pi^0$	$K\bar{K}^*$+c.c.
Br_{add}	0.0125	0.0057	0.0094	0.0013	0.0032	0.0009	0.0008	0.0084
mode	$K^*\bar{K}_2^*$+c.c.	$\omega f_2'$	ϕK^+K^-					
Br_{add}	0.0112	0.00053	0.00114					

$$\frac{1}{\sigma_{ggg}}\frac{d\sigma_{ggg}}{dx_1 dx_2}\simeq 2. \tag{5}$$

In order to simulate parton hadronization, the flavor generation machinery of the LUND model is applied for the $q\bar{q}$ fragmentation, and the LUND string model is applied for the gluon shower developing and fragmentation. Those parameters in JETSET7.4 which relate the ratios of baryon, pseudoscalar meson, vector meson, and tensor meson are tuned (shown in Table I). When the LUND model is applied at lower energies, for example in the charmonium region, some of the parameters in the model need to be adjusted. The minimum masses of the quark string and gluon string are decreased. According to the transverse momentum distribution of hadronic events observed in the BES experiment, the widths of the Gaussian distribution for the Px and Py are increased. Those tuned parameters are also listed in Table I.

B. Extended *C*- and *G*-parity conservation in the model

C- and *G*-parity conservation are not so important at higher energies; thus they are ignored in the LUND model. However, they are known to play important roles at lower energies in hadronic decay, so we include them into our generator.

C commutation is defined as an internal symmetry transformation of an interchanged particle and antiparticle. It is known that only a neutral nonstrange meson is an eigenstate of the unitary operator *C*, with an eigenvalue $+1$ or -1. The *C* parity of a neutral nonstrange meson is related to the spin J_i of the meson by $(-1)^{J_i}$ or $(-1)^{J_i+1}$. *C* parity is conserved in both electromagnetic interaction (i.e., decay to $q\bar{q}$ via a virtual photon) and strong interaction (i.e., decay via gluons). The *C* parity of a cluster of neutral mesons is assigned as $\Pi C_{neutral}$, the multiplication of those *C* parities of neutral mesons in the cluster. A charged particle is not the eigenstate of *C* commutation, and it is not assigned any *C* parity. However, a cluster system of charged particles can be assigned the *C* parity $C=(-1)^J$, depending on *J*, the angular momentum of the cluster system.

We liken the above *C* parity to a cluster system of charged mesons, strange mesons, and baryon particles. We assume that the contribution of the ith particle to the extended *C* parity of the cluster system is $(-1)^{J_i}$, where J_i is the spin of the ith particle:

$$C_{cluster}=\prod C_{neutral}\times(-1)^{int(\Sigma J_i)}. \tag{6}$$

We suppose a parameter R_J^i is the probability of whether the ith particle's contribution takes the value J_i or $J_i+1/2$. The parameter R_J^i of the antiparticle is identical to that of the particle.

The *G* commutation is defined as a complex transformation which first performs a rotation through π around the second axis in the isotopic-spin space, and then performs a *C* transformation. The *G* parity of the nonstrange meson is $(-1)^I C$, where *I* is the isotopic spin of the meson. In our model, *G*-parity conservation is handled in a way similar to *C*-parity conservation. The differences between the *G* parity and *C* parity are that the *G* parity is conserved only during strong interaction, and both the neutral and charged nonstrange mesons are eigenstates of the *G* operator. The *G* parity of a cluster of nonstrange mesons is denoted $\Pi G_{non\text{-}strange}$, the multiplication of these *G* parities of nonstrange mesons in the cluster. The strange meson and the baryon are not eigenstates of *G* commutation, and they are not assigned *G* parities. We liken the *G* parity to a cluster system, and we assume that it can be assigned an extended *G* parity as $(-1)^I C$, where *I* is the isotopic spin of the cluster system, and *C* is its *C* parity. In our generator, the extended *G* parity of the multiparticle cluster system is denoted

$$G_{cluster}=\prod G_{non\text{-}strange}\times(-1)^{int(\Sigma I_i)}C_i, \tag{7}$$

where I_i is the isotopic spin of the ith particle, and C_i is its extended *C* parity. The probability R_I^i is a parameter for the ith particle's contribution, which takes the value $(-1)^{I_i}$ or $(-1)^{I_i+1/2}$.

Values of above parameters R_J^i and R_I^i are obtained by fitting the branching ratios of the Monte Carlo sample to the experimental data. Their values are shown in Table II.

C. Abnormal suppression decay effect

J/ψ and $\psi(2S)$ decay into hadrons via three gluons or a virtual photon. According to perturbative QCD (PQCD), the 1^{2-} quarkonia decay width is given by Eq. (8) [15–17],

$$\Gamma(1^{2-}\rightarrow l^+l^-)\simeq 4e_q^2\alpha_e^2 m\frac{|R_{q\bar{q}}(0)|^2}{M_{q\bar{q}}}, \tag{8}$$

where e_q is the charge of the quark, $R_{q\bar{q}}(0)$ is the bound-state wave function at the origin, and $M_{q\bar{q}}$ is the mass of quarkonium. Also,

TABLE IV. Branching ratios of J/ψ decay.

			Decays into lepton					
Mode	B_{Expt}	B_{MC}	Mode	B_{Expt}	B_{MC}	Mode	B_{Expt}	B_{MC}
e^+e^-	6.02×10^{-2}	6.02×10^{-2}	$\mu^+\mu^-$	6.01×10^{-2}	6.0×10^{-2}			
Involving hadronic resonances			Decays into stable hadrons			Radiative decays		
Mode	Br_{Expt}	Br_{MC}	Mode	Br_{Expt}	Br_{MC}	Mode	Br_{Expt}	Br_{MC}
$\rho\pi$	1.27×10^{-2}	1.3×10^{-2}	$2(\pi^+\pi^-)\pi^0$	3.37×10^{-2}	3.4×10^{-2}	$\gamma\eta_c$	1.3×10^{-2}	1.3×10^{-2}
$\rho^0\pi^0$	4.2×10^{-3}	4.5×10^{-3}	$3(\pi^+\pi^-)\pi^0$	2.9×10^{-2}	3.6×10^{-2}	$\gamma\pi^+\pi^-2\pi^0$	8.3×10^{-3}	4.1×10^{-3}
$a_2\rho$	1.09×10^{-2}	1.2×10^{-2}	$\pi^+\pi^-\pi^0$	1.5×10^{-2}	1.8×10^{-2}	$\gamma\rho\rho$	4.5×10^{-3}	3.8×10^{-3}
ωf_2	4.3×10^{-3}	3.7×10^{-3}	$K^+K^-\pi^+\pi^-\pi^0$	1.2×10^{-2}	1.5×10^{-2}	$\gamma 2(\pi^+\pi^-)$	2.8×10^{-3}	2.0×10^{-3}
$b_1^\pm\pi^\mp$	3.0×10^{-3}	2.8×10^{-3}	$K^+K^-\pi^+\pi^-$	7.2×10^{-3}	6.9×10^{-3}	$\gamma\omega\omega$	1.59×10^{-3}	0.8×10^{-3}
$b_1^0\pi^0$	2.3×10^{-3}	1.6×10^{-3}	$K\overline{K}\pi$	6.1×10^{-3}	8.5×10^{-3}	$\gamma\phi\phi$	4.0×10^{-4}	2.5×10^{-3}
$K^{*0}\overline{K}_2^{*0}+$c.c.	6.7×10^{-3}	6.3×10^{-3}	$p\overline{p}\pi^+\pi^-$	6.0×10^{-3}	6.1×10^{-3}	$\gamma p\overline{p}$	3.8×10^{-4}	1.3×10^{-4}
$K^+\overline{K}^{*-}+$c.c.	5.0×10^{-3}	6.3×10^{-3}	$2(\pi^+\pi^-)$	4.0×10^{-3}	2.7×10^{-3}	$\gamma K\overline{K}$	9.7×10^{-4}	8.1×10^{-4}
$K^0\overline{K}^{*0}+$c.c.	4.2×10^{-3}	5.1×10^{-3}	$3(\pi^+\pi^-)$	4.0×10^{-3}	1.8×10^{-3}	$\gamma K\overline{K}\pi$	1.7×10^{-3}	2.8×10^{-3}
$\omega\pi^0\pi^0$	3.4×10^{-3}	3.9×10^{-3}	$n\overline{n}\pi^+\pi^-$	4.0×10^{-3}	8.7×10^{-3}			
$\omega K^*\overline{K}+$c.c.	5.3×10^{-3}	7.6×10^{-3}	$\Sigma^0\overline{\Sigma}^0$	1.27×10^{-3}	1.9×10^{-3}			
$\phi K^*\overline{K}+$c.c.	2.04×10^{-3}	6.6×10^{-3}	$K^+K^-2(\pi^+\pi^-)$	3.1×10^{-3}	7.1×10^{-3}			
$\Delta^{++}\overline{p}\pi-$	1.6×10^{-3}	1.8×10^{-3}	$p\overline{p}\pi^+\pi^-\pi^0$	2.3×10^{-3}	7.5×10^{-3}			
$\omega\eta$	1.58×10^{-3}	1.6×10^{-3}	$p\overline{p}$	2.14×10^{-3}	2.7×10^{-3}			
$\phi K\overline{K}$	1.48×10^{-3}	2.2×10^{-3}	$p\overline{p}\eta$	2.09×10^{-3}	3.2×10^{-3}			
$p\overline{p}\omega$	1.3×10^{-3}	0.9×10^{-3}	$p\overline{n}\pi^-$	2.0×10^{-3}	1.7×10^{-3}			
$\Delta^{++}\overline{\Delta}^{--}$	1.1×10^{-3}	0.8×10^{-3}	$n\overline{n}$	1.9×10^{-3}	2.6×10^{-3}			
$\Sigma^{*-}\overline{\Sigma}^{*+}$	1.03×10^{-3}	0.6×10^{-3}	$\Xi\overline{\Xi}$	1.8×10^{-3}	1.9×10^{-3}			
$p\overline{p}\eta'$	9.0×10^{-4}	6.0×10^{-4}	$\Lambda\overline{\Lambda}$	1.35×10^{-3}	1.3×10^{-3}			
$\phi f_2'$	0.8×10^{-3}	1.6×10^{-3}	$p\overline{p}\pi^0$	1.09×10^{-3}	1.3×10^{-3}			
ωf_1	6.8×10^{-4}	5.6×10^{-4}	$\Lambda\overline{\Sigma}^-\pi^+$	1.06×10^{-3}	2.0×10^{-5}			
$\phi\eta$	6.5×10^{-4}	7.6×10^{-4}	$pK^-\overline{\Lambda}$	8.9×10^{-4}	8.1×10^{-4}			
$\Xi^{*-}\overline{\Xi}^+$	5.9×10^{-4}	3.0×10^{-4}	$2(K^+K^-)$	7.0×10^{-4}	1.5×10^{-3}			
$pK^-\overline{\Sigma}^{*0}$	5.1×10^{-4}	3.0×10^{-5}	$pK^-\overline{\Sigma}^0$	2.9×10^{-4}	3.0×10^{-5}			
$\omega\pi^0$	4.2×10^{-4}	1.2×10^{-3}	K^+K^-	2.37×10^{-4}	1.6×10^{-4}			
$\phi\eta'$	3.3×10^{-4}	6.0×10^{-4}	$\Lambda\overline{\Lambda}\pi^0$	2.2×10^{-4}	7.0×10^{-5}			
$\Xi^{*0}\overline{\Xi}^0$	3.2×10^{-4}	2.7×10^{-4}	$\pi^+\pi^-$	1.47×10^{-4}	9.0×10^{-4}			
$\Sigma^{*-}\overline{\Sigma}^+$	3.1×10^{-4}	8.9×10^{-4}						
$\rho\eta$	1.93×10^{-4}	3.0×10^{-4}						
$\omega\eta'$	1.67×10^{-4}	2.5×10^{-4}						
ωf_0	1.4×10^{-4}	5.2×10^{-4}						
$\rho\eta'$	1.05×10^{-4}	2.6×10^{-4}						
$a_2^\pm\pi^\mp$	$<4.3\times10^{-3}$	4.4×10^{-3}						
$K\overline{K}_2^*+c.c.$	$<4.0\times10^{-3}$	0.5×10^{-3}						
$K_2^{*0}\overline{K}_2^{*0}$	$<2.9\times10^{-3}$	0.9×10^{-4}						
$K^{*0}\overline{K}^{*0}$	$<5.0\times10^{-4}$	5.5×10^{-4}						
$p\overline{p}\rho$	$<3.1\times10^{-4}$	1.9×10^{-4}						
$\Sigma^{*0}\overline{\Lambda}$	$<2.0\times10^{-4}$	1.9×10^{-4}						
$\Delta^+\overline{p}$	$<1.0\times10^{-4}$	1.0×10^{-5}						
$\Sigma^0\overline{\Lambda}$	$<9.0\times10^{-5}$	1.3×10^{-3}						

TABLE V. Branching ratios of $\psi(2S)$ decay.

Mode	B_{Expt}	B_{MC}	Mode	B_{Expt}	B_{MC}	Mode	$B_{The.}$	B_{MC}
			Decays into lepton					
e^+e^-	8.5×10^{-3}	8.5×10^{-3}	$\mu^+\mu^-$	7.7×10^{-3}	7.7×10^{-3}	$\tau^+\tau^-$	3.15×10^{-3}	3.1×10^{-3}
Involving hadronic resonances			Decays into stable hadrons			Transition and Radiative		
Mode	Br_{Expt}	Br_{MC}	Mode	Br_{Expt}	Br_{MC}	Mode	Br_{Expt}	Br_{MC}
$\rho\pi$	$<8.3\times10^{-5}$	5.0×10^{-5}	$3(\pi^+\pi^-)\pi^0$	3.5×10^{-3}	5.9×10^{-3}	$J/\psi\pi^+\pi^-$	3.24×10^{-1}	3.24×10^{-1}
$a_2\rho$	$<2.3\times10^{-4}$*	2.1×10^{-4}	$2(\pi^+\pi^-)\pi^0$	3.0×10^{-3}	2.3×10^{-3}	$J/\psi\pi^0\pi^0$	1.84×10^{-1}	1.84×10^{-1}
ωf_2	$<1.7\times10^{-4}$*	0.0×10^{-5}	$K^+K^-\pi^+\pi^-$	1.6×10^{-3}	4.1×10^{-4}	$J/\psi\eta$	2.7×10^{-2}	2.7×10^{-2}
$b_1^{\pm}\pi^{\mp}$	5.2×10^{-4}*	2.5×10^{-4}	$K^+\overline{K}^{*0}\pi^-$ + c.c.	6.7×10^{-4}	1.3×10^{-4}	$J/\psi\pi^0$	9.7×10^{-4}	9.7×10^{-4}
$K^{*0}\overline{K}_2^{*0}$ + c.c.	$<1.2\times10^{-4}$*	6.0×10^{-5}	$p\overline{p}\pi^+\pi^-$	8.0×10^{-4}	1.3×10^{-3}	$\gamma\chi_{c0}$	9.3×10^{-2}	9.2×10^{-2}
$K^+\overline{K}^{*-}$ + c.c.	$<5.4\times10^{-5}$	1.6×10^{-4}	$p\overline{p}$	1.9×10^{-4}	2.6×10^{-4}	$\gamma\chi_{c1}$	8.7×10^{-2}	8.7×10^{-2}
$\phi f_2'$	$<4.5\times10^{-5}$*	2.0×10^{-5}	$3(\pi^+\pi^-)$	1.5×10^{-4}	1.7×10^{-4}	$\gamma\chi_{c2}$	7.8×10^{-2}	7.2×10^{-2}
$\Xi^-\overline{\Xi}^+$	2×10^{-4}	1.5×10^{-4}	$p\overline{p}\pi^0$	1.4×10^{-4}	1.4×10^{-4}	$\gamma\eta_c$	2.8×10^{-3}	2.7×10^{-3}
			$\pi^+\pi^-$	8×10^{-5}	7×10^{-5}	$J/\psi\mu^+\mu^-$	1.0×10^{-2}	1.0×10^{-2}
			$\pi^+\pi^-\pi^0$	8.0×10^{-5}	3.2×10^{-4}			
			$2(\pi^+\pi^-)$	4.5×10^{-4}	1.4×10^{-4}			
			K^+K^-	1.0×10^{-4}	2×10^{-5}			
			$K^+K^-\pi^0$	$<2.96\times10^{-5}$	6.0×10^{-5}			
			$K_1\overline{K}$	1.0×10^{-3}*	1.6×10^{-4}			
			$K_1^*\overline{K}$	$<3.1\times10^{-4}$*	3.0×10^{-5}			

$$\Gamma(1^{2-}\to ggg)\simeq\frac{10}{9\pi^2}(\pi^2-9)\alpha_s^3\frac{|R_{q\overline{q}}(0)|^2}{M_{q\overline{q}}}, \tag{9}$$

where α_s is the strong-coupling constant. From Eqs. (8) and (9), the branching ratios of J/ψ and $\psi(2S)$, decaying into hadrons via ggg, have the relation

$$Q_h=\frac{B[\psi(2S)\to ggg]}{B(J/\psi\to ggg)}\simeq\frac{B[\psi(2S)\to e+e^-]}{B(J/\psi\to e^+e^-)}. \tag{10}$$

Inputting the data from PDG [9], we obtain $Q_h\simeq 0.15$. J/ψ and $\psi(2S)$ decay into hadrons via the virtual photon following the same relation. For most decay modes Eq. (10) holds, but some abnormal suppression modes have been found by the Mark II Collaboration; this suppression is known as the $\rho\pi/K^*\overline{K}$ puzzle [18].

In recent years, more and more abnormal suppression modes have been found by BES experiments in charmonium decaying into vector-pseudoscalar mesons, as well as vector-tensor mesons [19–22]. Various theories have been presented to explain this abnormal suppression phenomenon [23–28].

In order to handle these abnormal suppression modes, we suppose that $\psi(2S)$ decays normally, while we add the abnormal decay modes in J/ψ decay according to Eq. (11),

$$\mathrm{Br}(J/\psi)_{add}=\mathrm{Br}(J/\psi)_{Expt}-\frac{\mathrm{Br}[\psi(2S)]_{Expt}}{0.15}, \tag{11}$$

where Br_{Expt} is the experimental branching ratio from the PDG [8–10] and BES [19–22].

All abnormal suppression modes can be handled by the above method, except the $\rho\pi$ mode. The $\rho\pi$ mode cannot be suppressed by C- and G-parity conservation; however it is known to be suppressed strongly in $\psi(2S)$ decay. In order to reproduce $\rho\pi$ mode suppression, we first assume that the $\rho\pi$ mode is strongly suppressed ($\sim$90%) both in J/ψ and $\psi(2S)$ decays, and then add the experimentally measured branching ratio into the J/ψ decay. All the branching ratios added into the J/ψ decay are shown in Table III.

III. COMPARISON BETWEEN MONTE CARLO SIMULATION RESULTS AND EXPERIMENTAL DATA

With our model, J/ψ and $\psi(2S)$ inclusive decays are simulated. Tables IV and V are the results of J/ψ and $\psi(2S)$ decays. In Tables IV and V, most experimental data are from the PDG [8–10], and the rest from the BES [19–22]; these latter are marked by an asterisk.

As we pointed out in Sec. II, charmonium decay modes can be divided into two categories according to whether they are completely measured or not. From modes of charmonium decay through transitions, and modes of charmonium decay into leptons listed in Tables IV and V, it is shown that the branching ratios are the same as the input value, and this means that our generator works self-consistently.

As to the modes of the second category, they are simulated by the method described in Sec. II. The results are in Tables IV and V. It can be seen that most branching ratios

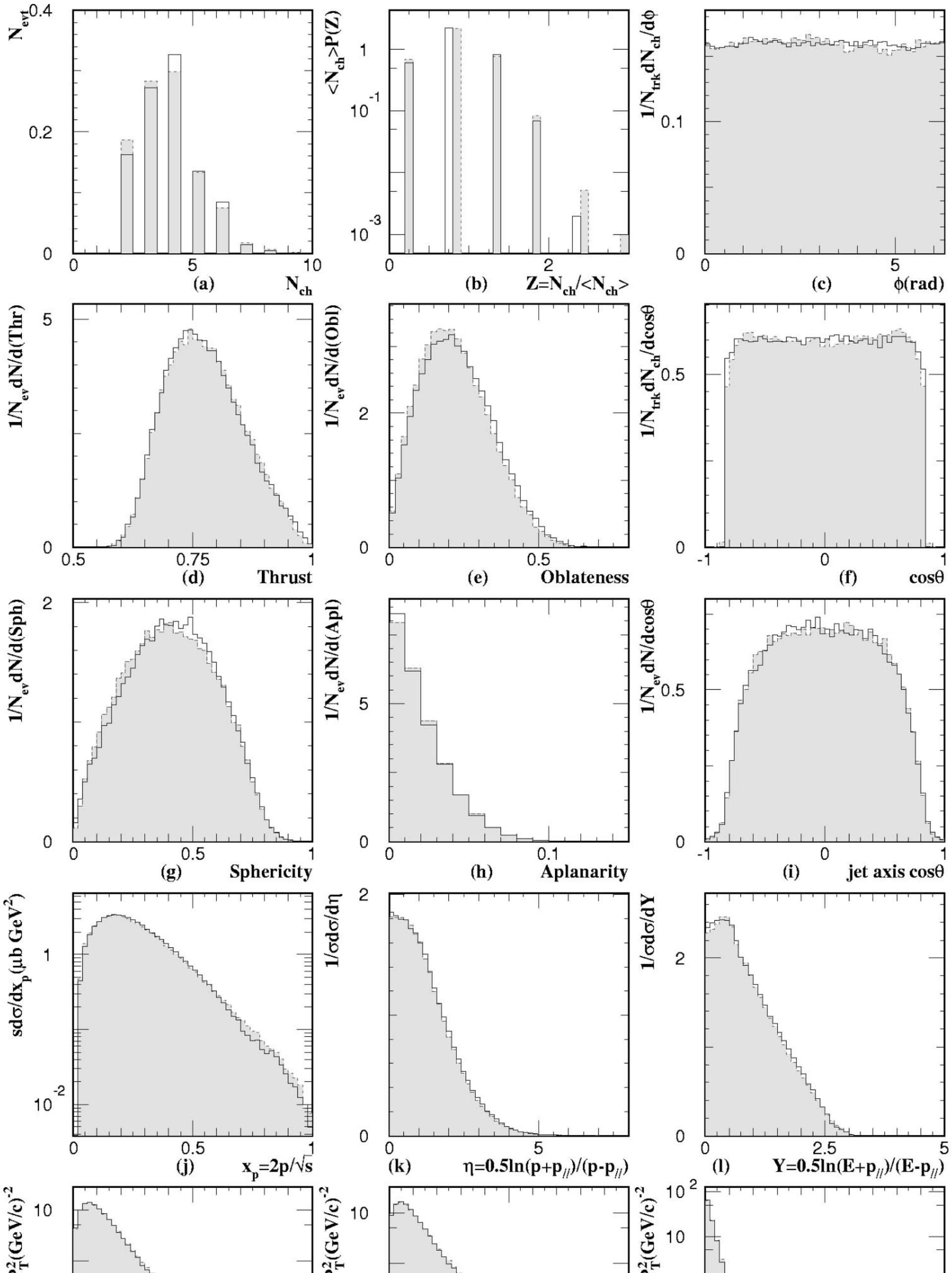

FIG. 2. Global properties of hadronic events produced in the J/ψ decay. In the figure, shadows are the distribution of BES experimental data, lines are those generated by our generator. (a) The charged multiplicity of events, N_{ch}; (b) the KNO scaling [30]; (c) the azimuthal angle ϕ distribution of charged particles; (d) the sphericity distribution [31]; (e) aplanarity distribution; (f) polar angle cos θ distribution of charged particles; (g) thrust distribution [32,33]; (h) oblateness distribution; (i) jet axes polar angle cos θ_J distributions of events [34]; (j) the distribution of Feynman scaling variable; (k) pseudorapidity; (l) rapidity; (m) transverse momentum of charged particles; (n) projection of p_T in the jet injection plane; and (o) p_T projection out of the jet injection plane.

are consistent with experimental data. Not only are the branching ratios of stable hadrons or radiative products reproduced, but the branching ratios of charmonium decays involving hadronic resonance are consistent with the experimental data as well. Both final products and intermediate states of charmonium decay are simulated satisfactorily by our generator.

Properties of hadronic events can be described by distributions of their kinematic variables. Figures 2 and 3 depict distributions of variables of hadronic events from the J/ψ and $\psi(2S)$ decays. In these figures, shadows show distributions by experimental data from the BES, and lines are the Monte Carlo sample generated by our model. The BES data used here are about 200000 events collected in 1993 for the study of J/ψ, and about 1600000 events collected in 1995 for $\psi(2S)$. Hadronic events were selected recently by the BES for criteria in the R scan [29]. About 100000 hadronic events with at least two charged tracks were selected from the J/ψ

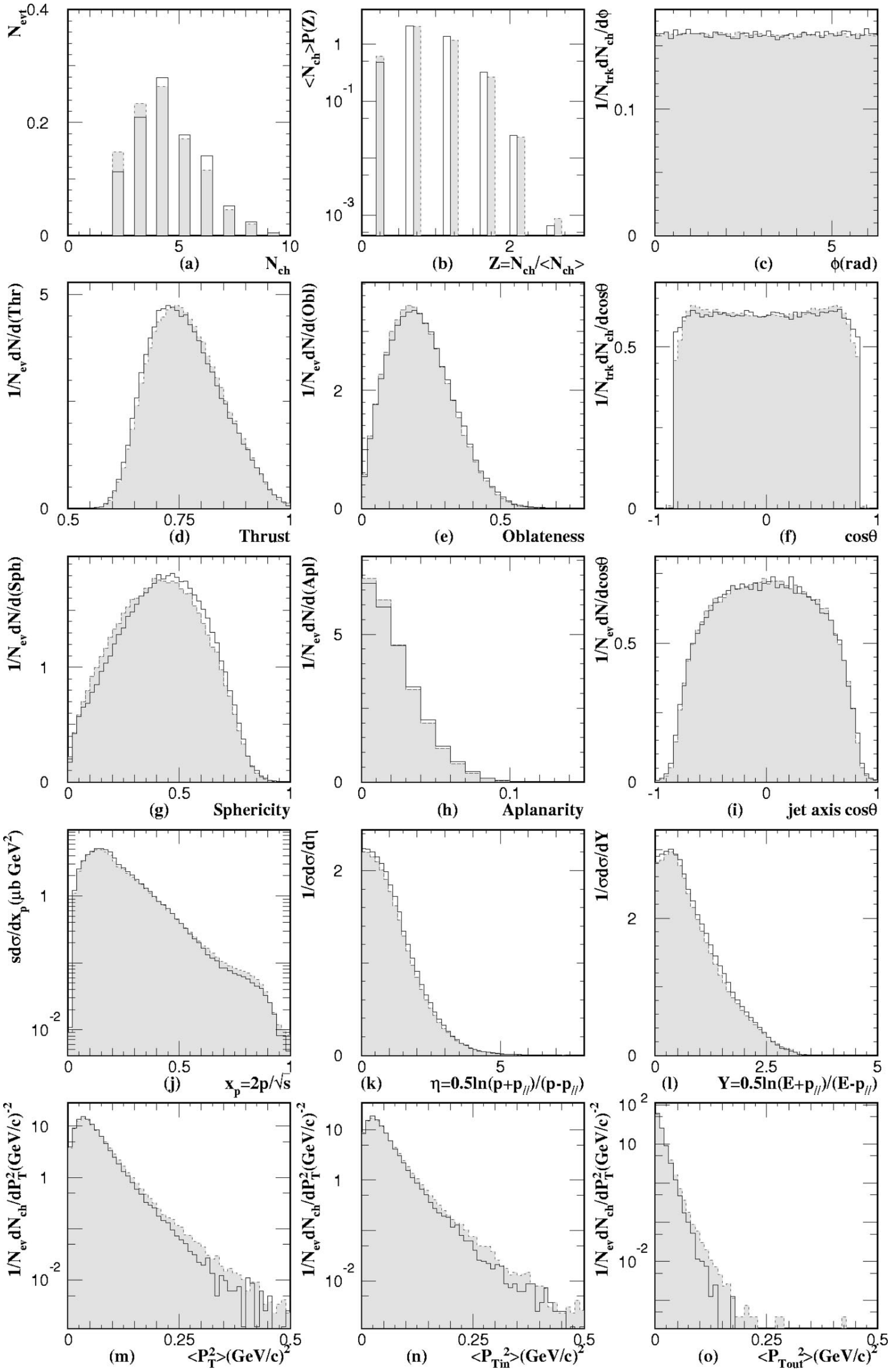

FIG. 3. Global properties of hadronic events produced in the $\psi(2S)$ decay. Shadows are the distribution of BES experimental data, and lines are those generated by our generator.

sample, and 260000 hadronic events were selected from the $\psi(2S)$ sample.

In Figs. 2 and 3, (a) is the charged multiplicity of events N_{ch}; (b) is the KNO scaling distribution [30]; (c) is the azimuthal angle ϕ distribution; (d) and (e) are the sphericity and aplanarity distribution of events [31], which show the features of the partonic jet of the event; (f) is the $\cos\theta$ distribution of charged particles, where θ is the polar angle; (g), (h), and (i) are the thrust [32,33], oblateness, and jet axes polar angle $\cos\theta_J$ distribution of events [34]; and (j) is the distribution of the Feynman scaling variable. In addition, kinematic properties of events are depicted by pseudorapidity (k), rapidity (l), and transverse momentum distributions [(m), (n), and (o)].

In Figs. 2 and 3, it is shown that our model can fully reproduce the global properties of hadronic events in charmonium decay. Based on the consistency between the Monte Carlo sample and experimental data in the global properties of hadronic events, the acceptance can be calculated precisely for the process of charmonium decay into hadrons. This can improve the precision in the measurement of resonance widths of J/ψ and $\psi(2S)$, as well as the precision in the measurement of the total number of J/ψ or $\psi(2S)$ samples.

IV. CONCLUSION

We presented a new model of charmonium inclusive decay. We treated the charmonium decays by two categories. The first consists of decays which have been fully measured, such as decays into leptons and into other charmoniums via transition. They are simulated simply by including their well-measured branching ratios into the generator. The second category consists of inclusive decays which are not well measured, such as decay into hadrons via $q\bar{q}$ or $\gamma gg/ggg$. These are simulated by our model. In our model, gluons shower development are handled by the LUND string model, and unstable particle decays are handled by the codes of JETSET7.4. In addition, extended *C*- and *G*-parity conservations are assumed. The abnormal suppressive decay modes observed in the experiments are handled by first presuming that $\psi(2S)$ decays normally, and then adding those abnormal modes into the J/ψ decay.

We simulated J/ψ and $\psi(2S)$ inclusive decays satisfactorily. The Monte Carlo results are consistent with experimental data in various properties, such as branching ratios involving hadronic resonances, stable hadrons, or radiative products, as well as global properties of hadronic events. We expect our generator will contribute to an improvement of the precision in the measurement of branching ratios of charmonium decays.

ACKNOWLEDGMENTS

The authors would like to express their appreciation to Dr. Xinhua Li, who proposed this work and who provided us with some helpful suggestions. We thank Dr. Torbjorn Sjostrand, Professor B. Andersson, and Dr. Tai An for helping us to apply the LUND model in the BES experiment, P. Wang for modifying our manuscript, and H. M. Hu for providing useful suggestions. The authors would like to express much thanks to all the members of the BES Collaboration; the BES data and BES software are the results of their hard work. We especially thank Professor Z. G. Zhao and B. S. Cheng and all of the other members of the R group, the M.C. group, and the $\psi(2S)$ group of the BES, for their various helpful discussions and contributions.

[1] E. Eichten *et al.*, Phys. Rev. Lett. **34**, 369 (1975).
[2] E. Eichten *et al.*, Phys. Rev. D **17**, 3090 (1978).
[3] L. M. Jones *et al.*, Phys. Rev. D **17**, 2332 (1978).
[4] K. Koller and T. F. Walsh, Nucl. Phys. **B140**, 449 (1978).
[5] W. Kwong *et al.*, Phys. Rev. D **37**, 3210 (1988).
[6] V. A. Novilov *et al.*, Phys. Rep. **41**, 1 (1978).
[7] B. Andersson, G. Gustafson, and T. Sjostrand, Z. Phys. C **6**, 235 (1980); T. Sjostrand, Comput. Phys. Commun. **27**, 243 (1982); **82**, 74 (1994).
[8] Particle Data Group, R. Burnett *et al.*, Phys. Rev. D **54**, 1 (1996).
[9] Particle Data Group, C. Caso *et al.*, Eur. Phys. J. C **3**, 1 (1998).
[10] Y. F. Gu and X. H. Li, Phys. Lett. B **449**, 361 (1999).
[11] R. D. Field, Phys. Lett. **133B**, 248 (1983).
[12] Guido Altarelli, Phys. Rep. **81**, 1 (1982).
[13] K. Koller and T. F. Walsh, Phys. Lett. **72B**, 227 (1977).
[14] S. J. Brodsky, G. P. Lepage, and P. B. Mackenzie, Phys. Rev. D **28**, 228 (1983).
[15] T. Applequist and D. Polizter, Phys. Rev. Lett. **34**, 43 (1975).
[16] R. Barbieri, R. Gatto, and R. Kogerler, Phys. Lett. **60B**, 183 (1976).
[17] R. Barbieri, R. Gatto, and R. Remiddi, Phys. Lett. **61B**, 368 (1976).
[18] M. E. B. Franklin *et al.*, Phys. Rev. Lett. **51**, 963 (1983).
[19] BES Collaboration, High Energy Phys. Nucl. Phys. **19**, 93 (1995).
[20] BES Collaboration, High Energy Phys. Nucl. Phys. **20**, 481 (1996).
[21] BES Collaboration, High Energy Phys. Nucl. Phys. **21**, 89 (1997).
[22] BES Collaboration, J. Z. Bai *et al.*, Phys. Rev. Lett. **81**, 5080 (1998).
[23] S. J. Brodsky, G. P. Lepage, and S. F. Tuan, Phys. Rev. Lett. **59**, 621 (1987).
[24] Wei-Shu Hou and A. Soni, Phys. Rev. Lett. **50**, 569 (1983).
[25] M. Chaichian *et al.*, Nucl. Phys. **B323**, 75 (1989).
[26] S. S. Pinsky, Phys. Lett. B **236**, 479 (1990).
[27] S. J. Brodsky and M. Karliner, Phys. Rev. Lett. **78**, 4682 (1997).
[28] X. Q. Li, D. V. Bugg, and B. S. Zhou, Phys. Rev. D **55**, 1421 (1997).
[29] BES Collaboration, Phys. Rev. Lett. **84**, 594 (2000).
[30] Z. Koba, H. B. Nielsen, and P. Olesen, Nucl. Phys. **B40**, 317 (1972).
[31] J. D. Bjorken and S. J. Brodsky, Phys. Rev. D **1**, 1416 (1970).
[32] S. Brandt *et al.*, Phys. Lett. **12**, 57 (1964).
[33] E. Fahri, Phys. Rev. Lett. **39**, 187 (1977).
[34] R. Marshall, 1989, RAL-89-021, 3.10-3.17.